Preprints.org

Article

Intranasal Trans-Sialidase Vaccine Mitigates Acute and Chronic Pathology in a Preclinical Oral Chagas Disease Model

Maria Florencia Pacini , Camila Bulfoni Balbi , Brenda Dinatale , Cecilia Farre , Paula Cacik , Florencia Belén Gonzalez , Ivan Marcipar , Ana Rosa Pérez [*]

Article

Intranasal Trans-Sialidase Vaccine Mitigates Acute and Chronic Pathology in a Preclinical Oral Chagas Disease Model

Maria Florencia Pacini [1], **Camila Bulfoni Balbi** [1], **Brenda Dinatale** [1], **Cecilia Farré** [1,2], **Paula Cacik** [3], **Florencia Belén Gonzalez** [1], **Iván Marcipar** [3] and **Ana Rosa Pérez** [1,2,*]

[1] Instituto de Inmunología Clínica y Experimental de Rosario (IDICER-CONICET), Argentina; pacini@idicer-conicet.gob.ar (M.F.P); bulfonibalbi@idicer-conicet.gob.ar (C.B.B.); dinatale@idicer-conicet.gob.ar (B.D.); farre@idicer-conicet.gob.ar (C.F.)

[2] Centro de Investigación y Producción de Reactivos Biológicos (CIPReB), Facultad de Ciencias Médicas, Universidad Nacional de Rosario, Argentina; farre@idicer-conicet.gob.ar (C.F.)

[3] Laboratorio de Tecnología Inmunológica, Facultad de Bioquímica y Ciencias Biológicas, Universidad Nacional del Litoral, Argentina; paula.cacik@gmail.com (P.C.)   imarcipr@fbcb.unl.edu.ar (I.M.)

[*] Correspondence: perez@idicer-conicet.gob.ar; +54 93416511301.

Abstract: Chagas disease, caused by *Trypanosoma cruzi*, leads to severe complications in 30% of infected individuals, including acute myocarditis and chronic fibrosing cardiomyopathy. Despite the significant burden of the disease, there is currently no licensed vaccine available to prevent it. This study aimed to evaluate the mucosal and systemic immunogenicity as well as the prophylactic efficacy of a mucosal vaccine and its impact on both acute and chronic cardiomyopathy. The results showed that nasal administration of Trans-sialidase (TS) plus c-di-AMP (TS+A). TS+A vaccine elicited NALT expression of IFN-γ, IL-17a, and IL-4 mRNA, and nasal-specific IgA production. Ex vivo challenge with TS also triggered enhanced proliferation of lymphocyte from the NALT, sentinel cervical lymph node and spleen. TS+A immunization increased plasma levels of Th1/Th2/Th17 cytokines and an evident cellular response to judge enhanced delayed-type hypersensitivity responses following TS footpad challenge. After oral infection, TS+A-vaccinated mice showed significantly reduced parasitemia and parasite load in heart, muscle and intestine, while markers of hepatic and muscle damage as well as clinical manifestations of acute infection are strongly diminished. TS+A also attenuated acute myocarditis and heart expression of inflammatory markers. The protection conferred by TS+A extended into the chronic phase, where it resulted in a clear reduction in chronic myocarditis, fibrosis, and functional electrocardiographic abnormalities, associated with decreased expression of the pro-fibrotic TGF-β. These results revealed that it is possible to develop a mucosal vaccine against *T. cruzi* based on TS and c-di-AMP, capable to reduce the development of Chagas cardiomyopathy, the hallmark of Chagas disease.

Keywords: oral chagas disease; - chronic chagas cardiomyopathy - *Trypanosoma cruzi*; trans-sialidase - nasal vaccine - c-di-AMP

1. Introduction

Chagas disease, caused by the protozoan parasite *Trypanosoma cruz*i, continues to be a major public health challenge in Latin America. According to the World Health Organization, approximately 7 million people are currently infected across 21 countries in the region, with around 70 million individuals at risk of contracting the disease [1]. The infection leads to severe complications, including acute myocarditis and chronic fibrosing cardiomyopathy, which can result in heart failure, arrhythmias, and other life-threatening cardiac issues in about 30% of chronic case [2–5].

Although vector-borne transmission is the most recognized route, *Trypanosoma cruzi* can also spread through congenital transmission, organ transplantation, blood transfusion, and, increasingly, through oral transmission [4,6,7]. Evidence suggests that oral infection often presents with more severe symptoms compared to vector-borne transmission, even in adults. The past few decades have seen a marked increase in cases of acute Chagas disease linked to oral infection, contributing to a rise in fatalities from acute cardiomyopathy [8,9].

Experimental vaccines against Chagas disease, typically administered via subcutaneous, intramuscular, or intradermal routes, aim to elicit robust systemic humoral and cellular responses to combat the parasite effectively. However, these studies showed no evidence of enhancing mucosal immunity, which, alongside the skin, is a primary entry point for *T. cruzi*. The potential of mucosal immunization has been relatively overlooked in Chagas disease research, despite its importance. Notably, the conjunctival mucosa, associated with the Romaña sign, and the buccal mucosa, often leading to facial edema in oral cases, are well-documented sites of natural human infection [10,11]. Experimental evidence further underscores the significance of mucosal entry points: the naso-maxillary region is a critical site for parasite entry following oral infection in mice, where the parasite persists and predominates for extended periods [12]. Similarly, studies on conjunctival mucosa infection revealed that parasites can drain through the nasolacrimal duct and subsequently infect the nasal cavity epithelium [13]. These findings, alongside previous research from our group [14], suggest that intranasal immunization with *T. cruzi*-derived antigens could effectively prevent parasite dissemination, regardless of the entry site (oral, other mucosal surfaces, or even skin). This approach could offer protection against both acute and chronic disease by inducing a comprehensive systemic and mucosal immune response.

Some members of the Trans-sialidase (TS) superfamily of *T. cruzi* proteins have been widely utilized as immunogens in various vaccine strategies, yielding promising results [15,16]. The active TSs, referred to as TS-Group I, are particularly immunodominant antigens in both mice and humans. These proteins exhibit enhanced efficacy as vaccine immunogens when their enzymatic activity is inhibited and the Shed Acute Phase Antigen (SAPA) domain is deleted, as the SAPA domain often acts as a decoy for the immune system [15]. Consequently, developing a recombinant vaccine based on an active TS fragment, in which the immunodominant SAPA repeats are removed while preserving the protein's overall structure, represents a promising strategy for enhancing vaccine efficacy against *Trypanosoma cruzi.*

In this context, we previously demonstrated that administering various recombinant fragments from active TS-based formulations via the oral or nasal routes offers distinct advantages over other methods, as it can elicit specific immune responses at both mucosal and systemic levels [14,17,18]. Importantly, while several preclinical vaccines tested so far have significantly reduced parasitemia during the acute phase, none have achieved sterilizing immunity, partly due to the complex life cycle of the parasite. Given the challenge of attaining sterilizing immunity, developing a vaccine that effectively reduces *T. cruzi* loads, prevents disease progression, or mitigates the severity of cardiac complications is crucial. Such a vaccine would improve the quality of life for individuals affected by Chagas disease by decreasing morbidity and mortality associated with cardiac issues, ultimately leading to a substantial reduction in the incidence of chronic chagasic cardiomyopathy and significantly alleviating the disease burden in endemic regions.

Chronic infection with the parasite *T. cruzi* leads to an inflammatory cardiomyopathy, resulting in scarring and significant alterations in cardiac structure, clinically referred to as Chronic Chagasic Cardiomyopathy (CCC) [19,20]. The invasion of parasites into cardiomyocytes recruits inflammatory cells, including macrophages, neutrophils, and CD4+ and CD8+ T cells, resulting in an inflammatory environment that is involved in the development of cellular hypertrophy [21,22]. Cytokines play a crucial role in regulating the immune response during the chronic phase of Chagas disease, aiding in infection control while also contributing to myocardial dysfunction [23]. While high levels of mRNA for both pro- and anti-inflammatory cytokines have been observed in mononuclear cells from patients chronically infected with *T. cruzi* [24], research indicates that cytokine production varies among patients with different clinical manifestations of the disease [24] . Inflammatory cytokines, like IFN-

γ and TNF-α, are associated with more severe clinical outcomes and the progression of CCC, while cytokines with a modulatory profile are linked to the maintenance of the indeterminate form, where cardiac and digestive functions remain largely unaffected. These findings underscore the importance of balancing pro- and anti-inflammatory immune profiles in the context of Chagas disease, suggesting that eliciting a balanced Th1/Th2/Th17 response could help control persistent parasites without exacerbating inflammatory or fibrotic damage in the host.

This study aimed to evaluate the immunogenicity and prophylactic efficacy of a nasally administered vaccine against oral *T. cruzi* infection, as well as its impact on both acute and chronic cardiomyopathy. The vaccine formulation tested included N-terminal recombinant fragments of a Group I trans-sialidase (TS), which lacks enzymatic activity and the immunodominant SAPA antigen, combined with bacterial dinucleotide c-di-AMP, known for its immunostimulatory properties at the nasal mucosa [25–28].

2. Materials and Methods

2.1. Expression and Purification of TS Recombinant Antigen

The N-terminal TS fragment was cloned and expressed in *E. coli* as previously described in Prochetto and col [29]. This fragment lacks enzymatic activity and SAPA antigen. Later, fragment purification was performed by affinity chromatography on Ni2+-NTA-agarose columns (InvitrogenTM, USA) with an imidazole/imidazole gradient of 8 M urea. All fractions were collected and dialyzed against PBS/0.5 M Urea and quantified by the bicinchoninic acid method. The presence of lipopolysaccharide (LPS) in the recombinant protein was determined using the Limulus Amebocyte Lysate (LAL test) kit (Genscript, USA). LPS levels were <10 endotoxin units (EU)/mg protein. The purity of the protein was checked by SDS-PAGE. The N-terminal fragment was indexed in GenBank with accession number MZ215730.

2.2. Mice

BALB/c female mice (6–8 weeks old) were obtained from the animal facilities of the Facultad de Ciencias Veterinarias de la Universidad Nacional de La Plata (LAE-FCV-UNLP) and kept in HEPA-ventilated cages at the facilities of the Centro de Investigación y Producción de Reactivos Biológicos, Facultad de Ciencias Médicas, Universidad Nacional de Rosario (CIPReB-FCM-UNR), both in Argentina. All protocols for animal studies were approved by the Institutional Animal Care & Use Committee (Res. Nro: 6698/2014 and No: 2958/2018), according to the Institutional guidelines and carried out following the National Institutes of Health guide for the care and use of Laboratory animals.

2.3. Immunization and Infection Protocol

Briefly, mice (4–7/group) were immunized intranasally with 3 doses (one every two weeks) of each formulation containing: a) Vehicle (saline solution, SS group); b) 10 μg of N-terminal TS fragment diluted in saline solution without any adjuvant (TS group); c) 10 μg of N-terminal TS fragment plus 5 μg of c-di-AMP (TS+A group); and d) Adjuvant alone as control group (A group). Two weeks after the last immunization, immunized animals were infected orally with a non-lethal dose of 2500 bloodstream trypomastigotes of Tulahuen strain (DTU-VI), maintained by serial passages in Cbi suckling mice (CIPREB-FCM-UNR). Parasitemia was monitored every 7 days by the examination of 5 mL of blood by direct microscopic evaluation, as previously described in Pacini et al. 2022 [14].

2.4. Determination of Specific Antibodies in Plasma and Nasal Lavages

Plasma was obtained by centrifugation at 5000 rpm of heparinized blood, which was subsequently stored at -20°C until total IgG, IgG2a, and IgG1 evaluation. To evaluate IgA in nasal secretions, nasal lavages were performed following the protocol reported by Cho and col [30]. Briefly, it was obtained by retrograde infusion through the trachea with 0.3 mL of cocktail containing

protease inhibitors (cOmplete™ Protease Inhibitor Cocktail, Roche, USA) and stored at -80 °C until use. For the detection of TS-specific antibodies, ELISA microplates (Nunc-Immuno MaxisorpTM, Thermo) were coated with the selected N-terminal fragment (0.5 µg/well) diluted in carbonate-bicarbonate buffer (0.05 M; pH 9.6). The procedure for determining plasma and nasal lavage antibodies was performed following the same protocol reported by Pacini et al. 2022 [14]. Briefly, samples were read at 450 nm with correction to 545 nm in an ELISA reader (Epoch Biotek Instruments, USA) after incubation with 100 µL of ready-to-use trimethylbenzidine (Wiener Lab, Argentina) followed by the addition of 50 µL of 2N H_2SO_4. (Wiener Lab, Argentina). Optical density (OD) values for Ig measurement were adjusted by subtracting the OD reading from the diluent (blank).

2.5. Delayed Type Hypersensitivity Test

A delayed-type hypersensitivity test (DHT) was performed by intradermal challenge with TS (5 µg of TS fragment) in the hind footpad of mice 15 days after the last immunization. Footpad swelling was measured with a digital calliper at 0, 24, 48, and 72 h post-challenge, as informed previously by Pacini and col [14].

2.6. Lymphocyte Culture and Flow Cytometry

After completing the immunization schedule, NALT, cervical lymph node (CLN) cells, and splenocytes were obtained by mechanical organ disaggregation in PBS+3%FBS (Gibco). Subsequently, 1×10^6 cells/well were cultured in 48-well plates (GBO) in DMEM medium supplemented with 10% FBS (Gibco), 2% penicillin (100 g/mL, Sigma), and streptomycin (100 U/mL, Sigma), either alone or stimulated with TS (10 µg/well). After 16 hours of culture, cells were incubated with anti-FcγII/III-R antibodies and stained with anti-CD4/PerCP, anti-CD8/PE, anti-B220/APC–Cy7, and anti-Ki67/FITC (all from BD Pharmingen) to determine lymphocyte proliferation. Samples were acquired using a BD FACSAria-II cytometer, with a minimum of 1×10^5 events acquired for each sample. FlowJo Software (Beckton-Dickinson, USA) was used for sample analysis.

2.7. Quantification of Plasma Cytokines

Plasma interleukin (IL)-2, IL-4, IL-6, IFN-γ, TNF-α, IL-17A, and IL-10 were quantified in samples obtained at -1, 17-, and 111-days post-infection (pi) by flow cytometry using the BD Cytometric Bead Array (BD Biosciences, USA), following the manufacturer's instructions. Samples were acquired on a BD FACSAriaII flow cytometer (Beckton-Dickinson, USA), and the concentrations of the cytokines of interest were determined using the BD-CBA software.

2.8. NALT and Heart Cytokine Profiling by RT-qPCR

The cytokine profile was analyzed in the NALT (day -1 pi) and heart (days 17 and 111 pi). Briefly, the NALT was isolated by carefully cutting the upper palate with a scalpel, following the inner contour of the mouse incisors and molars, and then gently peeling it off with forceps [31] and then the cells were extracted with TRI-Reagent®. Additionally, half a heart was removed and mechanically disrupted in TRI-Reagent®. The RNA was then reverse transcribed into cDNA using RevertAid Reverse Transcriptase (Thermo-Fisher Scientific, USA). Real-time PCR was performed on StepOnePlus equipment (Applied-Biosystems, USA) using Mix-5x-HOT-FIREPol®EvaGreen® qPCR-Mix Plus with ROX (Solis-BioDyne, Estonia). The amplification program included an initial activation step at 95ºC for 15 min, followed by denaturation at 95ºC for 15 s, annealing temperature between 59º/62ºC, and finally elongation at 72ºC for 20 s, for 40 cycles. Fluorescence was measured after each extension step and the specificity of the amplification was assessed by melting curve analysis. The GAPDH gene was used as a control to normalize the mRNA samples. Relative gene expression levels were calculated using an ad hoc standard curve for each gene. Amplification efficiencies were identical or similar between genes of interest and controls. The primers used were in Supp. Table 1 (ST1):

2.9. Clinical Score

To estimate the clinical impact of vaccine protective efficacy, we used a clinical scoring system developed by our group for non-lethal models of *T. cruzi* infection [14]. Briefly, the individual score was computed as the sum of the pre-established values for each clinical sign, as follows: absence of signs (0), piloerection (1), hunched posture (1.5), ocular involvement (2), decreased locomotor activity (2.5) and diarrhea (3). The overall score for each group/day was calculated as the average of individual scores. Finally, the cumulative score of each group was determined as the area under the curve (AUC).

2.10. Determination of Muscle and Liver Damage in the Acute and Chronic Phases

After infection, the activity of enzymes indicative of muscle and liver damage was assessed in fresh plasma: creatine kinase (CK), glutamate oxaloacetate transaminase (GOT), and glutamate pyruvate transaminase (GPT). These were measured using spectrophotometric tests, following the manufacturer's instructions (Roche).

2.11. Detection of Parasite Burden in Target Tissues

Heart, skeletal muscle and small intestine were collected for DNA extraction, following the method described in Cummings and Tarleton [32]. Briefly, total DNA was extracted from each sample after tissue disaggregation with a lysis buffer (10 mM Tris-HCl pH = 7.6; 0.1 M NaCl; 10 Mm EDTA; 0.5% SDS, 300 µg/ml proteinase K from Sigma). The samples were then heated for 2 h at 55 ◦C, and extracted twice with phenol:chloroform: isoamyl alcohol (25:24:1) (Sigma Chemical Co., St. Louis, MO). Cold ethanol (AAPER Alcohol and Chemical Co., Shelbyville, KY), twice the volume of the extracted sample, was then added and samples were placed at −80 ◦C for o.n. Samples were centrifuged for 30 min at 13,000 rpm and washed with 70% ethanol, vacuum dried and resuspended in sterile water. DNA samples were adjusted to a final concentration of 25 or 125 ng/µl and were used as a template for the qPCR reactions using the specific primers for *T. cruzi*: kDNA was amplified using S36 (5′GGT TCG ATT GGG GTT GGT G3′) and S67rev (5′GAA CCC CCC TCC CAA AAC C3′) primers. PCR reactions were performed using HOT FIREPol EvaGreen qPCR Mix Plus (Solis Biodyne) in StepOneTM Real-Time PCR Systems (Applied Biosystems) instrument. The parasite load was expressed as equivalent parasites in 50 ng of murine DNA.

2.12. Histopathology

Footpads (-1 day pi), hearts and sections of the quadriceps muscle (both at 17 and 111 days pi) were removed and fixed in 4% formalin and embedded in paraffin. Then 5 µm sections were stained with hematoxylin/eosin for evaluation of inflammatory infiltrates and cardiac and skeletal tissue damage, similar to that described in Pacini and col [14]. Additional sections of heart and skeletal muscle were stained with picrosirius red to evaluate tissue fibrosis. Fibrosis is classified based on the size and number of cardiac fibers affected as mild, moderate or severe. Taking these findings into account, a score was designed to quantify it. The slides were analyzed by an expert pathologist, who was blinded to the data.

2.13. Electrocardiograms

At 111 days pi, mice were anaesthetized with Ketamine (50%, Holliday-Scott S.A.)/Xylazine (10%, PharmaVet) solution and their cardiological function was subsequently monitored by electrocardiography. The recording of the electrocardiograms (ECG) was performed using an electrocardiograph specially designed for laboratory animals (Cardiocom, Argentina) and equipped with the CC7DerS-Vet software, supplied by the equipment manufacturer, which allows the evaluation of the heart rate (Fc) of each mouse and different parameters of cardiac functionality, such as the P wave, the PR interval, the PR segment, the QRS complex and the QT interval. As the value of the QT interval varies with the recorded Fc (decreases at high Fc and increases at low Fc), its value was corrected by applying the formula described in Mitchell et al., 1998 [33] to obtain the corrected

QT interval (QTc). Leads I and II were analyzed, and all alterations that showed some type of arrhythmia were recorded.

2.14. Statistical Analysis

Data were analyzed using non-parametric tests (ANOVA Kruskal-Wallis test (for k groups > 2), followed by Mann Whitney U test (for comparisons between two groups). Data were shown as mean±SEM or median/range depending on variable distribution. All analyzes were performed using GraphPad Instat 4.0 software (GraphPad, California, USA). Differences between groups were considered significant when the *p-value* was < 0.05.

3. Results

### 3.1. TS+A Recombinant Vaccine Elicits Both Mucosal and Systemic Immunogenicity

Fifteen days after completing the immunization schedule, the specific humoral immune response towards the N-terminal fragment of the catalytic domain of TS was analyzed, accompanied or not by the c-di-AMP (A) adjuvant (Figure 1). As shown in Figure 1a, animals immunized with the formulation containing TS+A showed a significant increase in total IgG compared to the groups receiving remaining formulations. The TS+A group also showed a substantial systemic response in terms of IgG2a and IgG1 (with an IgG2a/IgG1 ratio≈1, data not shown) (Figure 1b-c). In addition, the evaluation of nasal secretions indicated that mice immunized with TS+A presented increased levels of TS-specific IgA at the immunization site compared to the other groups. Animals vaccinated with the TS fragment alone showed similar values to those of SS and A (Figure 1a-d). To assess in vivo cell-mediated immunity, a delayed-type hypersensitivity (DTH) test was conducted on the footpads of mice. A pronounced swelling was revealed at 24 and 48 h post-challenge in the TS+A group (Figure 1e-f). Although it decreased by approximately 40% after 72 hours, it remained consistently elevated in the TS+A group compared to the others (Figure 1g). The DTH response induced in animals immunized with the TS fragment alone did not differ significantly from that observed in the SS group, indicating that the presence of di-AMP-c is necessary to induce the immunogenicity of the fragment. As seen in Figure 1h, the overall cellular response, measured as the area under the curve (AUC) from 0 to 72 hours, confirmed that only mice sensitized with TS+A triggered an evident specific cellular response against the N-terminal recombinant fragment. Histological analysis of the footpads at the peak of reactivity revealed an increase in immune cell infiltration, with greater intensity in the TS+A group (Figure 1i-j). The infiltrate mainly comprised polymorphonuclear cells in the SS group, while in contrast, mice immunized with TS, A, and TS+A exhibited a mixture of mononuclear and polymorphonuclear cells (Figure 1j). Notably, the TS+A group displayed predominantly mononuclear infiltration compared to the other groups. Mice administered with only the vehicle (without antigenic stimulus) showed no infiltration of any kind (Figure 1i-j). Globally, results of enhanced DTH reactivity recorded in the TS+A group showed a consistent clinical-histological concordance.

In the mucosa, the development of specific immune responses depends not only on the nature of antigenic stimulation but also in specialized inductive structures, such as NALT, and the subsequent expression of proinflammatory and immunoregulatory cytokines. Hence, to determine whether the formulation containing TS+A triggers in the NALT a particular cytokine profile, a wide range of cytokines associated with diverse immune patterns of response was evaluate by RT-qPCR. As can be observed in Figure 1k, mice immunized with TS+A displayed locally a significant increase in the expression of IFN-γ, IL-4, IL-5, IL-21 and IL-17a mRNA, compared to the SS, TS, and A groups, while no differences were found in IL-2 and IL-6 between groups. Similarly, plasma samples were evaluated to detect if nasal immunization elicits a specific cytokine pattern. As shown in Figure 1l, mice immunized with TS+A presented a slight but detectable increase of IFN-γ, IL-4, IL-17A, IL-6, and IL-2 in circulation compared with the rest groups. Although a tendency to increase IL-10 was also observed in the TS+A mice, this was not significant when compared to the rest of the groups

(Figure 1l). Conjointly, data showed that TS+A formulation triggers a mucosal and systemic pattern of cytokines linked to a better anti-*T. cruzi* immunogenic response.

Lastly, the proliferative potential of responding TS-specific lymphocytes was evaluated upon ex vivo restimulation with TS in NALT, CLN and spleen cells, following the gating strategy shown in Figure 1m. The proportion of CD4+, CD8+, and B220+ lymphocytes proliferating in response to TS (detected as Ki67+ cells) was similar to that of non-stimulated cells in the SS, TS, and A groups (Figure 1n-p). The proliferative response to TS was notably more evident in NALT, CLN, and spleen lymphocytes from mice vaccinated with TS+A compared to the other groups. Similarly, in the cells from the TS+A group exposed to TS, the proliferative response was higher than unstimulated cells, except for the CLN CD4+ T cells (Figure 1n-p). These results showed that TS+A formulation may trigger in both inductive and effector mucosal sites, as well as in a systemic secondary lymphoid organ, a critical recall response for controlling *T. cruzi*.
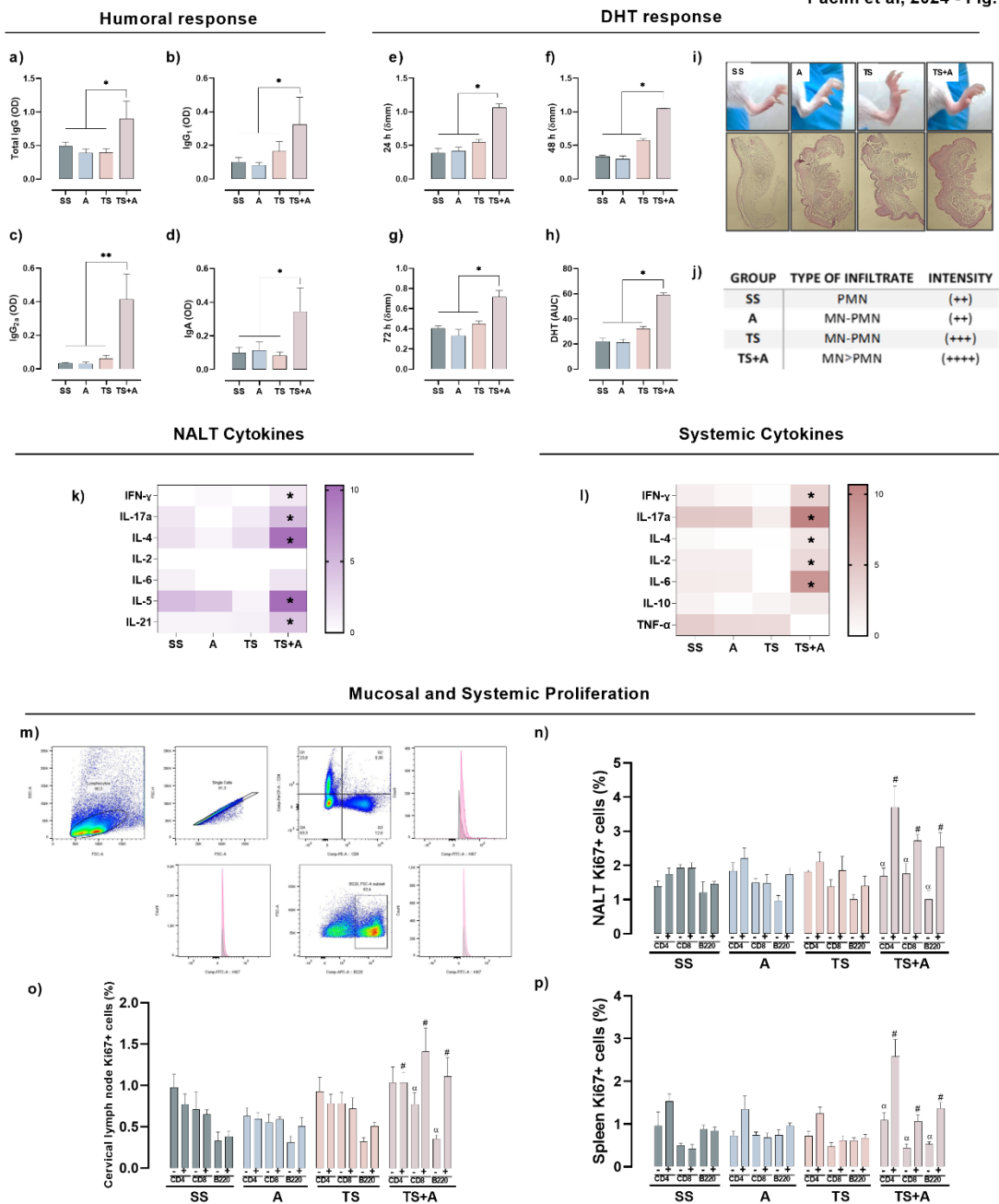
Figure 1. Mucosal and systemic immune response triggered by intranasal immunization. Fifteen days after completion of intranasal immunization, humoral and cellular response, as well as NALT and plasma cytokine patterns were evaluated. Humoral immune response: Plasma levels of: **a**) IgG, **b**) IgG2a, **c**) IgG1 and **d**) nasal IgA TS-specific antibodies by indirect ELISA and determination of optical density (OD) at 450/540 nm. Delayed type hypersensitivity test: Footpad thickness after intradermal injection of 5 µg of the N-terminal recombinant fragment of TS. The results are expressed as the difference between the value of the control footpad and that inoculated with TS (delta, Δ). Differences in thickness were obtained after: **e**) 24 h, **f**) 48 h, and **g**) 72 h. **h**) The area under the curve (AUC) corresponds to the interval from 0 to 72 h after re-exposure to the recombinant TS fragment. **i**) Representative images show footpad inflammation in each group after 24 h inoculation with the recombinant fragment. **j**) The panel shows the intensity of inflammation (the number of crosses indicates the degree of inflammation) and the type of infiltrate (PMN, polymorphonuclear; MN, mononuclear) after 48 h of challenge. NALT pattern of Th1, Th2, and Th17 cytokine expression: **k**) mRNA expression of typical cytokines of each of these profiles was evaluated by RT-qPCR and represented by heatmap. Plasma cytokines: **l**) IFN-γ, IL-4, IL-6, TNF-α, IL-2, IL10, and IL-17A were determined by CBA assay and represented by heatmap. The levels of significance are defined as follows: *$p < 0.05$ and **$p < 0.01$. Lymphoid cell proliferation in vaccinated mice: **m**) Gating strategy to estimate TS-specific proliferation after ex vivo restimulation with TS for 16 hours, followed by staining with Ki67 in **n**) NALT cells, **o**) Cervical lymph node cells and **p**) splenocytes. The levels of significance are defined as follows: α = $p < 0.05$ vs corresponding stimulated cells, # = $p < 0.05$ compared to stimulated cells of the rest groups.

3.2. Prophylactic TS+A Immunization Confers Protection during Acute Oral T. cruzi Infection

To assess the efficacy of the prophylactic nasal administration of TS-based formulations, mice were orally challenged with a sub-lethal dose of *T. cruzi* fifteen days after completing the immunization schedule. As shown previously [14], a sub-lethal model was selected to simulate what occurs in humans, where the infection is lethal in only a small proportion of infected individuals. First, the number of blood trypomastigotes and the clinical repercussion display during the acute phase were examined. Parasitemia peaks were recorded between two- and three-weeks pi and decreased progressively until they disappeared completely after six weeks pi, being in the TS+A group significantly lower than in the rest of the groups (Figure 2a). The improved control of circulating forms of *T. cruzi* accomplished in TS+A vaccinated mice was reflected by the 3-fold reduction in the cumulative parasitemia curve (AUC) compared to the SS group (Figure 2b). In infected animals, clinical signs began to appear around day 10 pi and disappeared after 60 days. However, animals immunized with TS+A exhibited a significant reduction in morbidity compared to those receiving other formulations, given clinical signs reverted after 36 days pi (Figure 2c). A cumulative assessment of the clinical impact of nasal vaccination showed a marked attenuation of acute signs of infection in TS+A immunized animals compared to the rest (Figure 2d).

Given the nature of the parasite strain used in this study (Tulahuen strain is reticulotropic but also myotropic) and the route of infection selected, a search for intracellular parasites was achieved in the heart, skeletal muscle and small intestine of immunized animals. In a similar way to what was observed with blood trypomastigotes, parasite burden in target tissues was strongly diminished in the TS+A immunized mice (Figure 2e-g). In addition, since parasitism can lead to tissue damage, the activity of enzymes acting as markers of heart, muscle, and liver tissue damage was also analyzed in immunized mice. An evident activity of creatinine kinase (CK), glutamate oxaloacetate transaminase (GOT), and glutamate pyruvate transaminase (GPT) (Figure 2h-j) was observed during the peak of parasitemia in the SS, TS, and A groups. Contrary, in the TS+A group, although CK only showed a slight increase, globally they did not differ from those observed in the NI control group. These results indicate the administration of TS+A prevented cardiac, muscle, and liver damage during the peak of parasitemia. In addition, when evaluated other systemic markers of inflammation, was observed that TNF-α and their counterregulatory cytokine IL-10 were significantly decreased in TS+A immunized mice concerning other groups, while no differences were found in terms of IFN-γ, IL-4, IL-6, IL-2, and IL-17A (Figure 2k). Moreover, histopathological studies of the heart indicated that the TS+A

vaccine provides cardiac protection, given mice immunized with TS+A showed little or no proportion and size of inflammatory foci in comparison to the other groups (Figure 2l-m). Moreover, 33% of TS+A immunized and infected animals show no evidence of myocarditis at day 17 pi (Figure 2m). These findings were reflected in the lowest score of histological findings recorded in the TS+A group (Figure 2n). Histological findings in the skeletal muscle were similar to those in the heart, showing large infiltrates affecting a large number of myocytes in the SS group, and on the contrary, small foci and attenuated damage in the TS+A group (Suppl. Figure 1). There is convincing evidence that cytokine networks can influence the clinical outcome of CD, for that we evaluated the levels and expression of various cytokines. Furthermore, hearts from TS+A vaccinated mice showed lower expression levels of TNF-α, TGF-β, MCP-1, iNOS, and Arg-II, while displaying contrasting levels of IL-17, compared to the SS group at day 17 pi (Figure 2o). A similar behavior was also observed in the TS group regarding TNF-α and TGF-β (Figure 2o). No significant differences in IL-10, IFN-γ, IL-1β, IL-6 and iNOS expression were found among groups (Figure 2o). These findings collectively demonstrate that nasal mucosa administration of TS+A, exhibits not only high efficacy in parasite control but also in mitigating both inflammatory markers and tissue damage, thereby contributing to a favorable course during the acute phase following oral *T. cruzi* infection.

Pacini et al, 2024 - Fig. 2
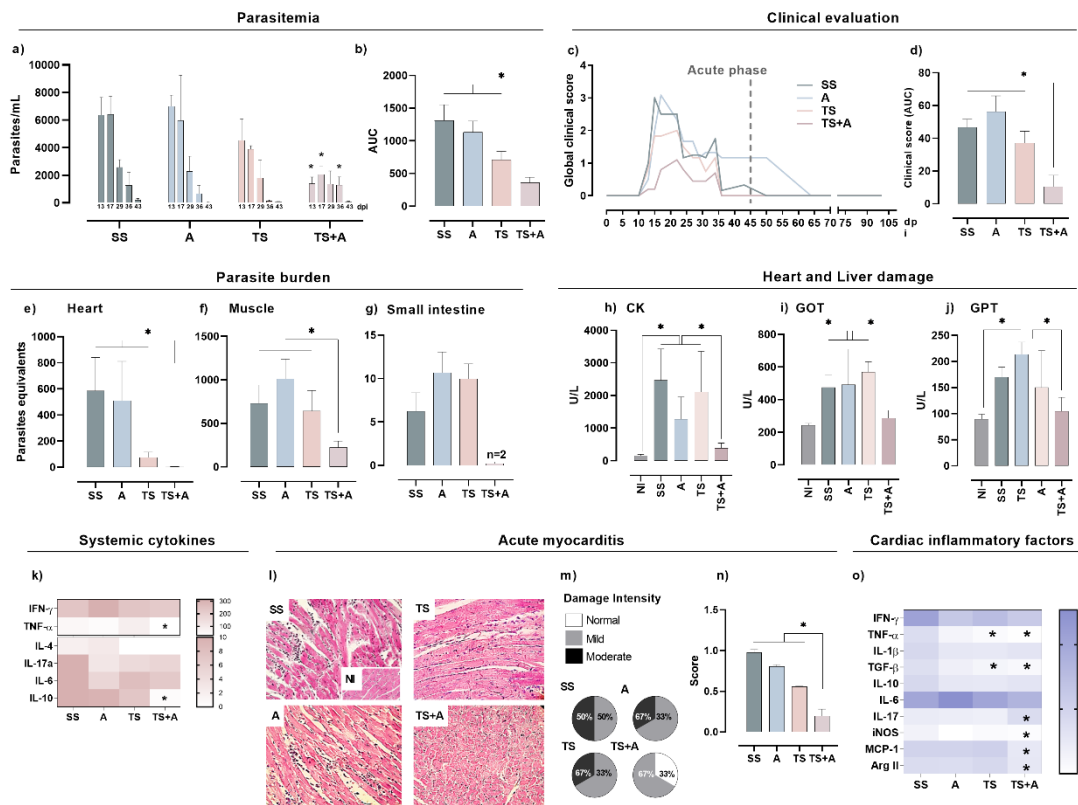
Figure 2. Vaccine efficacy in the acute phase. Animals were orally infected with 2500 trypomastigotes (Tulahuen strain) fifteen days after completing immunization. Parasitemia**: a**) The presence of blood forms of parasites was determined by direct microscopy at different days post-infection (pi). **b**) The overall magnitude of infection was estimated as the area under the curve (AUC) of the parasitemia values obtained from day 0 to day 43 pi (right panel). Clinical evaluation: **c**) The clinical evolution of the immunized and infected mice was recorded daily. A previously developed clinical score based on the severity of signs of the acute disease was used to monitor the animals throughout the infection. Data are expressed as median values of each group/day. **d**) The global clinical involvement of each group was estimated as the area under the curve (AUC). Tissue parasite burden: **e**) heart, **f**) skeletal muscle, and **g**) small intestine tissues were analyzed to detect parasites at 17 dpi (n=5/group, except for TS+A, with a n=2). Plasma activity of heart, muscle, and liver damage-associated enzymes: **h**)

creatinine kinase (CK); **i**) glutamate oxaloacetate transaminase (GOT); and **j**) glutamate pyruvate transaminase (GPT) were evaluated in plasma samples from immunized and infected mice. Circulating cytokines: **k**) Heatmaps showing changes in the abundance of plasma cytokines after 17 dpi determined by flow cytometry. The intensity color is assigned according to the relative scale of expression. Acute myocarditis: Histological analysis was performed at day 17 pi. **l**) Representative images of cardiac tissues from immunized and orally infected animals. The smaller images inserted in the photograph corresponding to the SS group show normal tissue from an uninfected and unimmunized animal (40X magnification). **m**) Infiltrate intensities were classified as mild, moderate, or severe. Pie charts illustrate the proportion of animals within each group that exhibited each type of inflammatory infiltrate. **n**) Inflammatory score estimates the degree of tissue damage in each group based on the number and intensity of inflammatory infiltrates. Cardiac inflammatory factors: **o**) Heatmap showing heart cytokine expression during the acute phase in vaccinated and infected animals. Intensity color is assigned according to the relative scale of expression. *p < 0.05.

3.3. Prophylactic Immunization with TS+A Formulation Attenuates Chronic Chagasic Myocarditis and Heart Functional Abnormalities

To evaluate the impact of immunization on *T. cruzi*-induced changes in chronic cardiac function, ECG recordings were performed in anesthetized mice after 111 days post-infection. The evaluation of cardiac function revealed an increase in the magnitude of the QRS complex and the length of the QTc interval in the SS, TS, and A groups compared to the TS+A and NI groups (Figure 3a-b). Notably, both parameters were preserved in the TS+A group, with values comparable to those recorded in the NI group (Figure 3a-b). Furthermore, the proportion of animals exhibiting arrhythmias differed among the groups; 50% to 65% of animals in the SS, TS, and A groups had rhythm abnormalities, whereas this proportion was reduced to 40% in the TS+A group (data not shown).

After euthanasia, we analyzed systemic and cardiac cytokine levels, tissue parasite load, cardiac infiltrates, and fibrosis. The results revealed that TS+A immunized animals exhibited significant reductions in IL-10, TNF-α, and IFN-γ levels during the chronic phase, compared to the other groups (Figure 3c). No significant differences were found in IL-4, IL-6, IL-2, and IL-17A levels among the groups (Figure 3c). Additionally, the parasite burden in the heart and skeletal muscle was significantly lower in the TS+A and TS groups compared to the SS and A groups (Figure 3d-e).

To assess the impact of the vaccine formulations on *T. cruzi*-induced cardiac inflammation, we examined leukocyte infiltrates in cardiac tissue using H&E-stained sections. Mice immunized with TS+A exhibited a higher proportion of normal cardiac tissue (Figure 3f-g), whereas myocarditis scores were significantly elevated in mice from the SS, TS, and A groups compared to those in the TS+A group (Figure 3f). A similar trend was also observed in skeletal muscle tissue (Supp. Figure 1).

Additionally, heart cytokine expression in TS+A immunized mice showed a significant reduction in TGF-β compared to the SS group (TS+A vs SS, p<0.05), while no significant differences were observed in other cytokines among the groups (Figure 3j). Long-term infection with *T. cruzi* can lead to substantial fibrosis in cardiac tissues, as indicated by collagen fiber accumulation (Rossi et al., 2003). To evaluate collagen deposition, we analyzed picrosirius red-stained sections of heart tissues from chronically infected mice. Figures 3I and 3J illustrates that TS+A mice exhibited significantly reduced collagen deposition compared to the other groups. A similar reduction in collagen deposition was observed in the skeletal muscle (Supp. Figure 2). Collectively, these findings suggest that the TS+A vaccine formulation effectively reduces inflammatory cell infiltration into cardiac tissue, modulates the inflammatory response, and prevents the pathology associated with chronic *T. cruzi* infection.
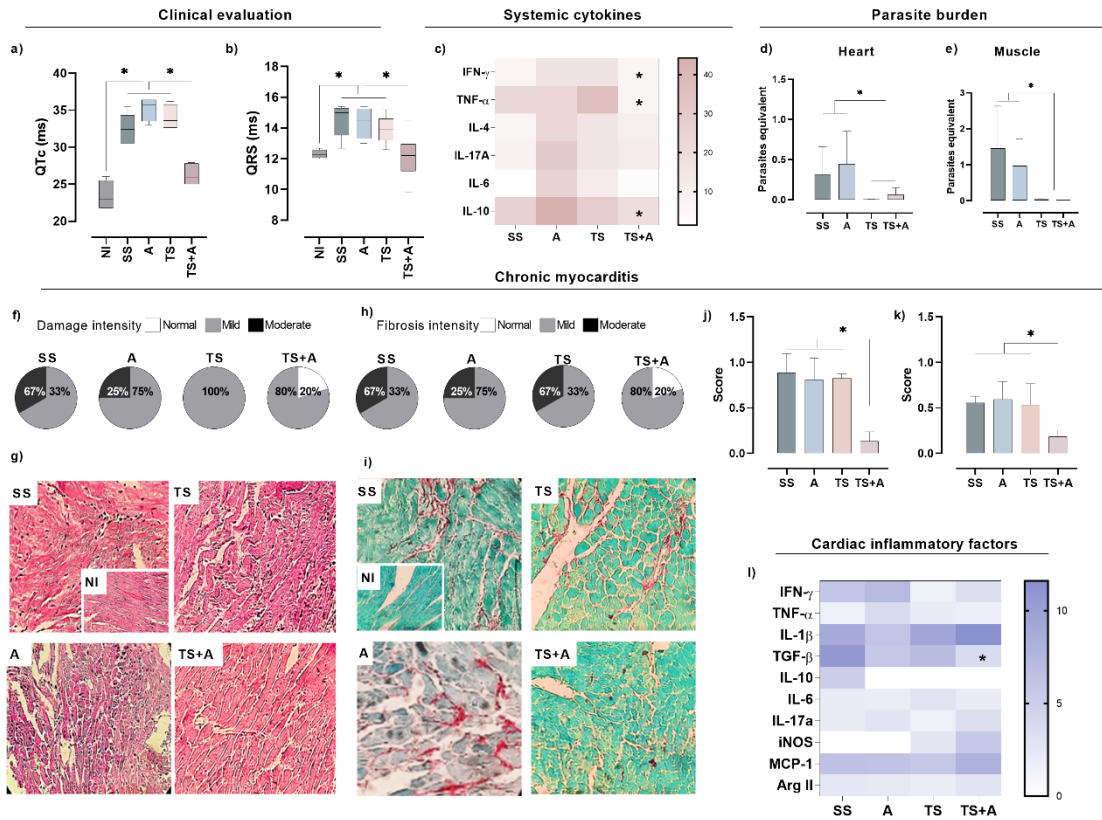
Figure 3. Vaccine efficacy in the chronic phase. Immunized and orally infected mice were evaluated after 111 days post-infection. Evaluation of cardiac function by ECGs in the chronic phase of infection, showing the corrected QT interval (**a**) and the QRS complex (**b**), both expressed in milliseconds. Systemic cytokines in immunized and chronically infected mice determined by CBA (**c**), represented as heatmap, where the intensity color is assigned according to the relative scale of expression. Cardiac (**d**) and skeletal muscle (**e**) parasite burden determined by qPCR. Evaluation of chronic myocarditis: histological sections of 5 μm cardiac tissue were stained with hematoxylin/eosin and picrosirius red. Chronic infiltrates and fibrosis were classified as mild, moderate, or severe. Pie charts show the relative proportion of each type of inflammatory infiltrate/group (**f**) or fibrosis (**g**). Images show representative histological findings in the cardiac tissue of immunized and orally infected animals: inflammatory infiltrates (**h**) and fibrosis (**i**). The smaller images inserted in the SS group show normal cardiac tissues from uninfected and non-immunized mice (magnification 40X), while bar graphs show the estimation of tissue damage based on the number and intensity of inflammatory infiltrates (**j**) or fibrosis (**k**). Heatmap showing heart cytokine expression in vaccinated and chronically infected animals (**l**), where the intensity color is assigned according to the relative scale of expression. CBA: Cytometric Bead Array. *$p<0.05$.

4. Discussion

In this study, we performed an in-depth immunological analysis to assess how mucosal administration of a prophylactic vaccine based on the N-terminal fragment of recombinant TS protects mice from oral *T. cruzi* infection. Our evaluation not only measured immunogenicity and vaccine's efficacy during the acute phase but also examined its long-term impact on the development of Chagas cardiomyopathy, a key manifestation of Chagas disease. Moreover, understanding the downstream signaling pathways activated by the recombinant TS fragment combined with c-di-AMP at the nasal mucosa and their role in mediating both oral and systemic immunity is crucial for elucidating how this vaccine formulation enhances anti-parasitic responses.

An effective approach for managing oral acute infection involves increasing both mucosal but also systemic TS-specific antibody production, and simultaneously, enhancing the cellular immune response. Given that the buccal mucosa, oropharynx, and palate serve as entry points for *T. cruzi* when parasites are deposited in the oral cavity [12], the presence of specific IgA in these surfaces can help prevent the parasites from adhering to and penetrating the epithelium. The elevated levels of TS-specific IgA observed at the immunization site in the TS+A group highlight the formulation's effectiveness in eliciting specific mucosal immunity, which may be crucial for controlling the early stages of oral infection. On the other hand, the systemic elevation of IgG2a and IgG1 indicates the development of a mixed Th1/Th2 immune profile, similar to what was observed with the C-terminal fragment of TS formulated with c-di-AMP [14]. Native active TS has been shown to skew the Th1/Th2 balance towards a Th2 response by reducing the production of IL-2, IL-13, and IFN-γ while increasing IL-4 levels, being this mechanism partly involved in the SAPA-driven parasite evasion of the immune response [34,35]. However, in our study, nasal administration of the TS fragment lacking the SAPA domain did not significantly elevate IL-4 levels in NALT, though TS+A did increase IL-4 levels in plasma. Moreover, cytokine profile triggered by TS+A is characterized by the presence of IFN-γ and IL-17A mRNA in the NALT and plasma. Similarly, intranasal immunization with a vaccine formulated with Tc52 (an antigen unrelated to the TS family) and c-di-AMP also induced IFN-γ and IL-17A secretion in T lymphocytes upon ex vivo re-stimulation [36]. These compartmentalization of cytokine production could help to improve the anti-parasite response [37]. A cytokine environment enriched with multiple cytokines particularly those produced by multifunctional Th1 cells involving the production of IFN-γ/IL-2/TNF-α has been linked with vaccine protective efficacy against various protozoan parasites, such as Leishmania, as well as viruses [38] and bacteria [39]. Despite TNF-α was not detected after TS+A administration, the vaccine triggered multiple cytokines at mucosal and systemic levels, including IFN-γ and IL-2, but also Th2 (IL-4/IL-5) and Th17 (IL-17) cytokines. TS+A also prompted the production of IL-6 and IL-21, cytokines critically involved in the follicular-Th (Tfh) differentiation and antibody production [40]. Numerous studies have demonstrated that c-di-AMP (as well as other dinucleotides), serve as highly effective immunopotentiator at the mucosal level, inducing a robust immune response characterized by a mixed Th1/Th2/Th17 profile [27]. This cytokine profile aligns with what we observed in our study and mirrors findings from other intranasally administered vaccines against *T. cruzi* combining recombinant peptides with c-di-AMP, such as those containing a C-terminal fragment of TS [18] or Tc52 [41]. Further supporting this, recent research with a subunit vaccine containing Ag85Bc plus c-di-AMP, administered intranasally to a mouse model of persistent *M. tuberculosis* H37Ra infection, also elicited a significantly enhanced Th1/Th2/Th17 response in the lungs and reduced pathological lesions [42]. Moreover, the p7 epitope, which is restricted by MHC-II and located in the N-terminal region of TS, has been associated with the induction of Th1 and Th17 lymphocytes in *T. cruzi* infection [43]. However, this epitope is absent in the fragment used in this study, as it is located between amino acids 23 to 43, while our fragment spans from 63 to 346. Taken together, these findings indicate that c-di-AMP, rather than the specific antigen, may be primarily responsible for driving this mixed cytokine pattern [27,44,45]. Additionally, the systemic and mucosal production of IL-17 may be partly mediated by TS-specific B lymphocytes, as demonstrated by Bermejo et al. in the context of *T. cruzi* infection [46]. Future studies involving various recombinant TS fragments adjuvanted with c-di-AMP will help elucidate the relative contributions of IL-17-producing Th17 and B cell populations in the vaccine's effectiveness.

The enhanced control of the parasite achieved with the TS+A vaccine after oral infection not only improved the clinical manifestations of the disease but also effectively collaborated in the prevention of tissue damage during the acute phase. This is evidenced by nearly baseline levels of CK, GOT, and GPT, along with minimal acute myocarditis observed in vaccinated animals. TNF-α is implicated in inflammatory cell trafficking and local tissue damage [47]; therefore, reduced plasma and heart TNF-α levels during the acute phase in the TS+A infected group are notably associated with cardiac protection. Moreover, other inflammatory cytokines are also diminished in hearts of TS+A acutely-infected mice, like TGF-β, INOS and MCP-1, supporting histological findings. More importantly, the vaccine's protective effect persisted into the chronic phase, with TS+A-immunized animals showing

fewer histological and electrical abnormalities, along with a reduced expression of TGF-β mRNA. In the context of pre-clinical and clinical studies of chronic Chagas disease, evidence indicates that TGF-β stimulates heart fibrosis and cardiac remodeling, and impairs heart conduction, contributing to a worse prognosis, while TGF-β inhibitors have been shown to reverse these effects [48,49], suggesting that the TS+A-induced reduction of this cytokine plays a crucial role in reducing fibrosis and supporting cardiac recovery. In addition, although chronic murine myocarditis may not perfectly mirror human chronic Chagas cardiomyopathy, BALB/c mice infected with Tulahuen exhibit clear electrocardiographic alterations, with QTc interval prolongation serving as a key indicator of histological damage [50], and justifies the use of ECG to assess the extent to which vaccine formulations can prevent or mitigate chronic myocarditis. Our results showed that while animals in the SS, TS, and A groups exhibited alterations in the QRS complex and QTc interval, those immunized with TS+A had values approaching those of the non-infected (NI) group. Additionally, the lower incidence of arrhythmias in the TS+A group suggests that this vaccine formulation effectively attenuates electrical conduction and repolarization abnormalities, particularly in the QTc interval. Prolonged QTc can indicate abnormal ventricular repolarization, which may result from cardiac autonomic dysfunction or inflammatory processes leading to fibrosis and myocardial dilation. Additionally, the administration of this formulation attenuated tissue lesions during the chronic phase of the experimental infection, which was associated with a decrease in abnormal electrical phenomena.

In this study, significant clinical effects are seen only when the selected TS fragment is combined with the c-di-AMP. However, it's important to consider several factors when evaluating the potential of this vaccine candidate. The variability among *T. cruzi* strains and the complexity of the parasite's life cycle might still pose challenges. The infective strain used in this study, Tulahuen, predominantly affects reticulocytes but also has myotropic properties and belongs to DTU VI. This lineage is known in South America for its association with myocarditis, along with DTU V [51–53]. Although the choice of Tulahuen was justified by its capacity to induce cardiac damage following oral infection [54], further research is needed to evaluate vaccine protection against other strains or DTUs, particularly those more frequently linked to oral infection outbreaks, such as DTU I and IV [55–57]. Despite that, the high sequence identity and conservation of antigenic regions within TS-GI proteins among different DTUs support their potential as broad-spectrum vaccine candidates [15]. Additionally, studies should explore the use of metacyclic trypomastigotes and assess the effectiveness of intranasal immunization against systemic challenges that better reflect vector-borne infection, such as subcutaneous or intradermal models. Additionally, the effectiveness of adjuvants like c-di-AMP needs to be validated across diverse populations and in different experimental models to ensure broad applicability. Further research should focus on evaluating how these findings translate to real-world scenarios and whether the observed protection is effective against various *T. cruzi* strains and at different stages of the disease. Additionally, assessing the long-term efficacy and safety of the vaccine through clinical trials will be crucial for its potential application in preventing Chagas disease.

Supplementary Materials: The following supporting information can be downloaded at the website of this paper posted on Preprints.org. Figure S1: Histopathological examination of skeletal muscle at day 17 pi; Figure S2: Histopathological examination of skeletal muscle at day 111 pi. Table S1: Primer sequences used for RT-qPCR.

Author Contributions: Conceptualization, A.R.P., M.F.P.; methodology and investigation, A.R.P., M.F.P., C.B.B., B.D., P.C., C.F., F.B.G.; formal analysis, A.R.P., I.M, M.F.P.; data curation, A.R.P., M.F.P.; writing—original draft preparation, A.R.P., M.F.P.; writing—review and editing, I.M., F.B.G.; supervision, A.R.P., I.M.; project administration, A.R.P.; resources and funding acquisition, A.R.P., I.M., F.B.G. All authors have read and agreed to the published version of the manuscript.

References

1. World Health Organization World Health Organization (2023) Chagas Disease (American Trypanosomiasis). Available online: https://www.who.int/chagas/en/.
2. Marin Neto, J.A.; Simões, M. V; Sarabanda, A. V Chagas' Heart Disease. *N. Engl. J. Med.* **2000**, *20*, 825–924.
3. H S Rassr, R.; Rassi, A.; L, W.C. Chagas' Heart Disease. *Clin. Cardiol* **2000**, *23*, 883–889.
4. Rassi, A.; Rassi, A.; Marin-Neto, J.A. Chagas Disease. *Lancet* **2010**, *375*, 1388–1402, doi:10.1016/S0140-6736(10)60061-X.
5. Bonney, K.M.; Luthringer, D.J.; Kim, S.A.; Garg, N.J.; Engman, D.M. Pathology and Pathogenesis of Chagas Heart Disease. *Annu. Rev. Pathol. Mech. Dis.* 2019.
6. Coura, J.R. Transmission of Chagasic Infection by Oral Route in the Natural History of Chagas Disease. *Rev. Soc. Bras. Med. Trop.* **2006**.
7. Rueda, K.; Trujillo, J.E.; Carranza, J.C.; Vallejo, G.A. Oral Transmission of Trypanosoma Cruzi : A New Epidemiological Scenario for Chagas' Disease in Colombia and Other South American Countries. *Biomedica* **2014**, doi:10.1590/S0120-41572014000400017.
8. Pereira, K.S.; Schmidt, F.L.; Guaraldo, A.M.A.; Franco, R.M.B.; Dias, V.L.; Passos, L.A.C. Chagas' Disease as a Foodborne Illness. *J. Food Prot.* 2009.
9. Filigheddu, M.T.; Górgolas, M.; Ramos, J.M. Orally-Transmitted Chagas Disease. *Med. Clínica (English Ed.* **2017**, doi:10.1016/j.medcle.2017.02.007.
10. Prata, A. Evolution of the Clinical and Epidemiological Knowledge about Chagas Disease 90 Years after Its Discovery. *Mem. Inst. Oswaldo Cruz* **1999**, doi:10.1590/S0074-02761999000700008.
11. de Noya, B.A.; González, O.N. An Ecological Overview on the Factors That Drives to Trypanosoma Cruzi Oral Transmission. *Acta Trop.* **2015**, doi:10.1016/j.actatropica.2015.06.004.
12. Silva-dos-Santos, D.; Barreto-de-Albuquerque, J.; Guerra, B.; Moreira, O.C.; Berbert, L.R.; Ramos, M.T.; Mascarenhas, B.A.S.; Britto, C.; Morrot, A.; Serra Villa-Verde, D.M.; et al. Unraveling Chagas Disease Transmission through the Oral Route: Gateways to Trypanosoma Cruzi Infection and Target Tissues. *PLoS Negl. Trop. Dis.* **2017**, doi:10.1371/journal.pntd.0005507.
13. Giddings, O.K.; Eickhoff, C.S.; Sullivan, N.L.; Hoft, D.F. Intranasal Vaccinations with the Trans-Sialidase Antigen plus CpG Adjuvant Induce Mucosal Immunity Protective against Conjunctival Trypanosoma Cruzi Challenges. *Infect. Immun.* **2010**, doi:10.1128/IAI.00278-09.
14. Pacini, M.F.; González, F.B.; Dinatale, B.; Bulfoni Balbi, C.; Villar, S.R.; Farré, C.; Lupi, G.; Espariz, M.; Blancato, V.S.; Magni, C.; et al. Nasal Immunization with a L. Lactis-Derived Trans-Sialidase Antigen plus c-Di-AMP Protects against Acute Oral T. Cruzi Infection. *Vaccine* **2022**, *40*, 2311–2323, doi:10.1016/J.VACCINE.2022.02.071.
15. Pacini, M.F.; Perdomini, A.; Bulfoni Balbi, C.; Dinatale, B.; Herrera, F.E.; Perez, A.R.; Marcipar, I. The High Identity of the Trypanosoma Cruzi Group-I of Trans-Sialidases Points Them as Promising Vaccine Immunogens. *Proteins Struct. Funct. Bioinforma.* **2023**, doi:10.1002/prot.26537.
16. Bontempi, I.; Fleitas, P.; Poato, A.; Vicco, M.; Rodeles, L.; Prochetto, E.; Cabrera, G.; Beluzzo, B.; Arias, D.; Racca, A.; et al. Trans-Sialidase Overcomes Many Antigens to Be Used as a Vaccine Candidate against Trypanosoma Cruzi. *Immunotherapy* **2017**, *9*, 555–565, doi:10.2217/imt-2017-0009.
17. Quintana, I.; Espariz, M.; Villar, S.R.; González, F.B.; Pacini, M.F.; Cabrera, G.; Bontempi, I.; Prochetto, E.; Stülke, J.; Perez, A.R.; et al. Genetic Engineering of Lactococcus Lactis Co-Producing Antigen and the Mucosal Adjuvant 3' 5'- Cyclic Di Adenosine Monophosphate (c-Di-AMP) as a Design Strategy to Develop a Mucosal Vaccine Prototype. *Front. Microbiol.* **2018**, doi:10.3389/fmicb.2018.02100.
18. Pacini, M.F.; Balbi, C.B.; Dinatale, B.; González, F.B.; Prochetto, E.; De Hernández, M.A.; Cribb, P.; Farré, C.; Espariz, M.; Blancato, V.S.; et al. Intranasal Trans-Sialidase-Based Vaccine against Trypanosoma Cruzi Triggers a Mixed Cytokine Profile in the Nasopharynx-Associated Lymphoid Tissue and Confers Local and Systemic Immunogenicity. *Acta Trop.* **2023**, doi:10.1016/j.actatropica.2023.106889.
19. Rossi, M.A.; Ramos, S.G.; Bestetti, R.B. Chagas' Heart Disease: Clinical-Pathological Correlation. *Front. Biosci.* 2003.

20. Álvarez, J.M.; Fonseca, R.; Borges Da Silva, H.; Marinho, C.R.F.; Bortoluci, K.R.; Sardinha, L.R.; Epiphanio, S.; D'Império Lima, M.R. Chagas Disease: Still Many Unsolved Issues. *Mediators Inflamm.* 2014.

21. Higuchi, M. de L.; De Brito, T.; Martins Reis, M.; Barbosa, A.; Bellotti, G.; Pereira-Barreto, A.C.; Pileggi, F. Correlation between Trypanosoma Cruzi Parasitism and Myocardial Inflammatory Infiltrate in Human Chronic Chagasic Myocarditis: Light Microscopy and Immunohistochemical Findings. *Cardiovasc. Pathol.* **1993**, 2, 101–106, doi:10.1016/1054-8807(93)90021-S.

22. Higuchi, M.D.L.; Reis, M.M.; Aiello, V.D.; Benvenuti, L.A.; Gutierrez, P.S.; Bellotti, G.; Pileggi, F. Association of an Increase in CD8+ T Cells with the Presence of Trypanosoma Cruzi Antigens in Chronic, Human, Chagasic Myocarditis. *Am. J. Trop. Med. Hyg.* **1997**, doi:10.4269/ajtmh.1997.56.485.

23. Bartekova, M.; Radosinska, J.; Jelemensky, M.; Dhalla, N.S. Role of Cytokines and Inflammation in Heart Function during Health and Disease. *Heart Fail. Rev.* 2018.

24. Koh, C.C.; Neves, E.G.A.; de Souza-Silva, T.G.; Carvalho, A.C.; Pinto, C.H.R.; Sobreira Galdino, A.; Gollob, K.J.; Dutra, W.O. Cytokine Networks as Targets for Preventing and Controlling Chagas Heart Disease. *Pathogens* 2023.

25. Burdette, D.L.; Monroe, K.M.; Sotelo-Troha, K.; Iwig, J.S.; Eckert, B.; Hyodo, M.; Hayakawa, Y.; Vance, R.E. STING Is a Direct Innate Immune Sensor of Cyclic Di-GMP. *Nature* **2011**, doi:10.1038/nature10429.

26. Lirussi, D.; Ebensen, T.; Schulze, K.; Trittel, S.; Duran, V.; Liebich, I.; Kalinke, U.; Guzmán, C.A. Type I IFN and Not TNF, Is Essential for Cyclic Di-Nucleotide-Elicited CTL by a Cytosolic Cross-Presentation Pathway. *EBioMedicine* **2017**, doi:10.1016/j.ebiom.2017.07.016.

27. Ebensen, T.; Libanova, R.; Schulze, K.; Yevsa, T.; Morr, M.; Guzm??n, C.A. Bis-(3',5')-Cyclic Dimeric Adenosine Monophosphate: Strong Th1/Th2/Th17 Promoting Mucosal Adjuvant. *Vaccine* **2011**, *29*, 5210–5220, doi:10.1016/j.vaccine.2011.05.026.

28. Madhun, A.S.; Haaheim, L.R.; Nøstbakken, J.K.; Ebensen, T.; Chichester, J.; Yusibov, V.; Guzman, C.A.; Cox, R.J. Intranasal C-Di-GMP-Adjuvanted Plant-Derived H5 Influenza Vaccine Induces Multifunctional Th1 CD4+ Cells and Strong Mucosal and Systemic Antibody Responses in Mice. *Vaccine* **2011**, doi:10.1016/j.vaccine.2011.04.094.

29. Prochetto, E.; Bontempi, I.; Rodeles, L.; Cabrera, G.; Vicco, M.; Cacik, P.; Pacini, M.F.; Pérez Gianeselli, M.; Pérez, A.R.; Marcipar, I. Assessment of a Combined Treatment with a Therapeutic Vaccine and Benznidazole for the Trypanosoma Cruzi Chronic Infection. *Acta Trop.* **2022**, *229*, doi:10.1016/J.ACTATROPICA.2022.106334.

30. Cho, S.H.; Oh, S.Y.; Zhu, Z.; Lee, J.; Lane, A.P. Spontaneous Eosinophilic Nasal Inflammation in a Genetically-Mutant Mouse: Comparative Study with an Allergic Inflammation Model. *PLoS One* **2012**, doi:10.1371/journal.pone.0035114.

31. Cisney, E.D.; Fernandez, S.; Hall, S.I.; Krietz, G.A.; Ulrich, R.G. Examining the Role of Nasopharyngeal-Associated Lymphoreticular Tissue (NALT) in Mouse Responses to Vaccines. *J. Vis. Exp.* **2012**, doi:10.3791/3960.

32. Cummings, K.L.; Tarleton, R.L. Rapid Quantitation of Trypanosoma Cruzi in Host Tissue by Real-Time PCR. *Mol. Biochem. Parasitol.* **2003**, doi:10.1016/S0166-6851(03)00093-8.

33. Mitchell, P.H.; Ferketich, S.; Jennings, B.M. Quality Health Outcomes Model. *J. Nurs. Scholarsh.* **1998**, doi:10.1111/j.1547-5069.1998.tb01234.x.

34. Díaz, P.R.; Mucci, J.; Meira, M.A.; Bogliotti, Y.; Musikant, D.; Leguizamón, M.S.; Campetella, O. Trypanosoma Cruzi Trans-Sialidase Prevents Elicitation of Th1 Cell Response via Interleukin 10 and Downregulates Th1 Effector Cells. *Infect. Immun.* **2015**, doi:10.1128/IAI.00031-15.

35. Nardy, A.F.F.R.; Freire-de-Lima, C.G.; Pérez, A.R.; Morrot, A. Role of Trypanosoma Cruzi Trans-Sialidase on the Escape from Host Immune Surveillance. *Front. Microbiol.* **2016**, *7*, doi:10.3389/fmicb.2016.00348.

36. Cai, C.W.; Eickhoff, C.S.; Meza, K.A.; Blase, J.R.; Audette, R.E.; Chan, D.H.; Bockerstett, K.A.; DiPaolo, R.J.; Hoft, D.F. Th17 Cells Provide Mucosal Protection against Gastric Trypanosoma Cruzi Infection. *Infect. Immun.* **2021**, *89*, doi:10.1128/IAI.00738-20.

37. De Meis, J.; Morrot, A.; Farias-de-Oliveira, D.A.; Villa-Verde, D.M.S.; Savino, W. Differential Regional Immune Response in Chagas Disease. *PLoS Negl. Trop. Dis.* 2009.

38. Morales-Sánchez, A.; Fuentes-Pananá, E.M. Human Viruses and Cancer. *Viruses* 2014.

39. Ning, H.; Zhang, W.; Kang, J.; Ding, T.; Liang, X.; Lu, Y.; Guo, C.; Sun, W.; Wang, H.; Bai, Y.; et al. Subunit Vaccine ESAT-6:C-Di-AMP Delivered by Intranasal Route Elicits Immune Responses and Protects Against Mycobacterium Tuberculosis Infection. *Front. Cell. Infect. Microbiol.* **2021**, doi:10.3389/fcimb.2021.647220.

40. Eto, D.; Lao, C.; DiToro, D.; Barnett, B.; Escobar, T.C.; Kageyama, R.; Yusuf, I.; Crotty, S. IL-21 and IL-6 Are Critical for Different Aspects of B Cell Immunity and Redundantly Induce Optimal Follicular Helper CD4 T Cell (Tfh) Differentiation. *PLoS One* **2011**, doi:10.1371/journal.pone.0017739.

41. Matos, M.N.; Cazorla, S.I.; Schulze, K.; Ebensen, T.; Guzm??n, C.A.; Malchiodi, E.L. Immunization with Tc52 or Its Amino Terminal Domain Adjuvanted with C-Di-AMP Induces Th17+Th1 Specific Immune Responses and Confers Protection against Trypanosoma Cruzi. *PLoS Negl. Trop. Dis.* **2017**, *11*, 1–16, doi:10.1371/journal.pntd.0005300.

42. Liang, X.; Cui, R.; Li, X.; Ning, H.; Kang, J.; Lu, Y.; Zhou, S.; Huang, X.; Peng, Y.; Zhang, J.; et al. Ag85B with C-Di-AMP as Mucosal Adjuvant Showed Immunotherapeutic Effects on Persistent Mycobacterium Tuberculosis Infection in Mice. *Brazilian J. Med. Biol. Res.* **2024**, *57*, 1–10, doi:10.1590/1414-431X2024e13409.

43. Acevedo, G.R.; Girard, M.C.; Gómez, K.A. The Unsolved Jigsaw Puzzle of the Immune Response in Chagas Disease. *Front. Immunol.* 2018.

44. Sanchez Alberti, A.; Bivona, A.E.; Cerny, N.; Schulze, K.; Weißmann, S.; Ebensen, T.; Morales, C.; Padilla, A.M.; Cazorla, S.I.; Tarleton, R.L.; et al. Engineered Trivalent Immunogen Adjuvanted with a STING Agonist Confers Protection against Trypanosoma Cruzi Infection. *npj Vaccines* **2017**, *2*, 9, doi:10.1038/s41541-017-0010-z.

45. Sanchez Alberti, A.; Bivona, A.E.; Matos, M.N.; Cerny, N.; Schulze, K.; Weißmann, S.; Ebensen, T.; González, G.; Morales, C.; Cardoso, A.C.; et al. Mucosal Heterologous Prime/Boost Vaccination Induces Polyfunctional Systemic Immunity, Improving Protection Against Trypanosoma Cruzi. *Front. Immunol.* **2020**, doi:10.3389/fimmu.2020.00128.

46. Bermejo, D.A.; Jackson, S.W.; Gorosito-Serran, M.; Acosta-Rodriguez, E. V.; Amezcua Vesely, M.C.; Sather, B.D.; Singh, A.K.; Khim, S.; Mucci, J.; Liggitt, D.; et al. Trypanosoma Cruzi Trans-Sialidase Initiates a Program Independent of the Transcription Factors RORγt and Ahr That Leads to IL-17 Production by Activated B Cells. *Nat. Immunol.* **2013**, doi:10.1038/ni.2569.

47. Pérez, A.R.; Berbert, L.R.; Lepletier, A.; Revelli, S.; Bottasso, O.; Silva-Barbosa, S.D.; Savino, W. TNF-α Is Involved in the Abnormal Thymocyte Migration during Experimental Trypanosoma Cruzi Infection and Favors the Export of Immature Cells. *PLoS One* **2012**, doi:10.1371/journal.pone.0034360.

48. Ferreira, R.R.; Waghabi, M.C.; Bailly, S.; Feige, J.J.; Hasslocher-Moreno, A.M.; Saraiva, R.M.; Araujo-Jorge, T.C. The Search for Biomarkers and Treatments in Chagas Disease: Insights From TGF-Beta Studies and Immunogenetics. *Front. Cell. Infect. Microbiol.* 2022.

49. Saraiva, R.M.; Waghabi, M.C.; Vilela, M.F.; Madeira, F.S.; Da Silva, G.M.S.; Xavier, S.S.; Feige, J.J.; Hasslocher-Moreno, A.M.; Araujo-Jorge, T.C. Predictive Value of Transforming Growth Factor-B1in Chagas Disease: Towards a Biomarker Surrogate of Clinical Outcome. *Trans. R. Soc. Trop. Med. Hyg.* **2013**, doi:10.1093/trstmh/trt050.

50. Eickhoff, C.S.; Lawrence, C.T.; Sagartz, J.E.; Bryant, L.A.; Labovitz, A.J.; Gala, S.S.; Hoft, D.F. ECG Detection of Murine Chagasic Cardiomyopathy. *J. Parasitol.* **2010**, doi:10.1645/GE-2396.1.

51. Guhl, F.; Ramírez, J.D. Retrospective Molecular Integrated Epidemiology of Chagas Disease in Colombia. *Infect. Genet. Evol.* **2013**, doi:10.1016/j.meegid.2013.08.028.

52. Zingales, B.; Andrade, S.G.; Briones, M.R.S.; Campbell, D.A.; Chiari, E.; Fernandes, O.; Guhl, F.; Lages-Silva, E.; Macedo, A.M.; Machado, C.R.; et al. A New Consensus for Trypanosoma Cruzi Intraspecific Nomenclature: Second Revision Meeting Recommends TcI to TcVI. *Mem. Inst. Oswaldo Cruz* **2009**, *104*, 1051–1054, doi:10.1590/S0074-02762009000700021.

53. Burgos, J.M.; Diez, M.; Vigliano, C.; Bisio, M.; Risso, M.; Duffy, T.; Cura, C.; Brusses, B.; Favaloro, L.; Leguizamon, M.S.; et al. Molecular Identification of Trypanosoma Cruzi Discrete Typing Units in End-Stage Chronic Chagas Heart Disease and Reactivation after Heart Transplantation. *Clin. Infect. Dis.* **2010**, doi:10.1086/655680.

54. Barreto-de-Albuquerque, J.; Silva-dos-Santos, D.; Pérez, A.R.; Berbert, L.R.; de Santana-van-Vliet, E.; Farias-de-Oliveira, D.A.; Moreira, O.C.; Roggero, E.; de Carvalho-Pinto, C.E.; Jurberg, J.; et al. Trypanosoma Cruzi Infection through the Oral Route Promotes a Severe Infection in Mice: New Disease Form from an Old Infection? *PLoS Negl. Trop. Dis.* **2015**, *9*, doi:10.1371/journal.pntd.0003849.

55. de Freitas, V.L.T.; Piotto, M.R.; Esper, H.R.; Nakanishi, E.Y.S.; Fonseca, C. de A.; Assy, J.G.P.L.; Berreta, O.C.P.; França, F.O. de S.; Lopes, M.H. Detection of Trypanosoma Cruzi DTUs TcI and TcIV in Two Outbreaks of Orally-Transmitted Chagas Disease in the Northern Region of Brazil. *Rev. Inst. Med. Trop. Sao Paulo* **2023**, doi:10.1590/S1678-9946202365007.

56. Ramírez, J.D.; Montilla, M.; Cucunubá, Z.M.; Floréz, A.C.; Zambrano, P.; Guhl, F. Molecular Epidemiology of Human Oral Chagas Disease Outbreaks in Colombia. *PLoS Negl. Trop. Dis.* **2013**, doi:10.1371/journal.pntd.0002041.

57. Monteiro, W.M.; Magalhães, L.K.C.; de Sá, A.R.N.; Gomes, M.L.; Toledo, M.J. de O.; Borges, L.; Pires, I.; Guerra, J.A. de O.; Silveira, H.; Barbosa, M. das G.V. Trypanosoma Cruzi IV Causing Outbreaks of Acute Chagas Disease and Infections by Different Haplotypes in the Western Brazilian Amazonia. *PLoS One* **2012**, doi:10.1371/journal.pone.0041284.